

# Spin-polarized transport through a quantum dot coupled to ferromagnetic leads: Kondo correlation effect

Jing Ma, Bing Dong, and X. L. Lei

*Department of Physics, Shanghai Jiaotong University, 1954 Huashan Road, Shanghai 200030, China*  
(June 5, 2018)

We investigate the linear and nonlinear transport through a single level quantum dot connected to two ferromagnetic leads in Kondo regime, using the slave-boson mean field approach for finite on-site Coulomb repulsion. We find that for antiparallel alignment of the spin orientations in the leads, a single zero-bias Kondo peak always appears in the voltage-dependent differential conductance with peak height going down to zero as the polarization grows to  $P = 1$ . For parallel configuration, with increasing polarization from zero, the Kondo peak descends and greatly widens by the appearance of shoulders, and finally splits into two peaks on both sides of the bias voltage around  $P \sim 0.7$  until disappears at even larger polarization strength. At any spin orientation angle  $\theta$ , the linear conductance generally drops with growing polarization strength. For a given finite polarization, the minimum linear conductance always appears at  $\theta = \pi$ .

72.15.Qm, 73.23.Hk, 73.40.Gk, 73.50.Fq

## I. INTRODUCTION

Since the discovery of the giant magnetoresistance effect,<sup>1</sup> extensive theoretical and experimental attention has been paid to the spin-dependent electron transport through systems consisting of two ferromagnetic layers (FM) sandwiched by a nonmagnetic structure of different types, including insulator,<sup>2</sup> semiconductor quantum well,<sup>3</sup> carbon nanotube,<sup>4</sup> and composite structure.<sup>5</sup> Quite a lot interesting spin related transport effects and device functions have been predicted, observed, even realized. These investigations constitute an important part of the rapidly developing field of magnetoelectronics or spin-electronics.<sup>6</sup> Recently, FM/quantum-dot(QD)/FM system has attracted much attention. Different from previously studied nonmagnetic structure, a quantum dot features the strong many-body correlation among electrons in it such that, not only the Coulomb blockade can dominate its electronic transport, but, particularly, a significant Kondo effect may arise when it connects to normal leads, exhibiting zero-bias maximum in the differential conductance in the cases when odd number of electrons resides in. It is of course interesting to see what happens when the normal metal leads are replaced by ferromagnetic leads. How is the Kondo-correlated state affected by the strength and the relative orientation of the spin polarizations of two magnetic leads?

In a recent paper, Sergueev *et al.*<sup>7</sup> presented a theoretical analysis of the transport characteristics of such a FM/QD/FM system modeled by the Anderson single-impurity Hamiltonian with finite Coulomb repulsion  $U$ , using the ansatz proposed by Ng<sup>8</sup> and the standard equation-of-motion technique for the retarded Green's function with the usual decoupling procedure for the higher order functions. They found that there is always a sharp single Kondo resonant peak in nonlinear differential conductance at zero bias and that the height of the peak exhibits only a modest change with varying

the polarization strength from 0 to 0.6 and with varying the spin orientation angle from 0 to  $\pi$ . Very recently, markedly different results were reported on similar systems in the  $U \rightarrow \infty$  limit by two groups,<sup>9,10</sup> based also on the equation-of-motion technique together with Ng's ansatz<sup>8</sup> or with some kind of additional assumption to determine renormalized level of the QD. They found that for parallel alignment of the lead magnetizations, the Kondo resonance peak in the differential conductance splits at a polarization value as small as 0.2.

In this paper we investigate the spin-polarized transport through a quantum dot coupled to ferromagnetic leads using a finite- $U$  slave-boson mean-field (SBMF) approach of Kotliar and Ruckenstein.<sup>11</sup> As an effective nonperturbative technique, different versions of SBFM method<sup>12,11</sup> have been used to study the equilibrium and out-of-equilibrium Kondo effect in a single QD and double QDs connected to normal leads without and with a magnetic field.<sup>13-17</sup> It is generally believed that the SBFM approach is reliable in describing the Kondo regime at low temperature but may have problem to deal with strong charge fluctuations.<sup>15</sup> Nevertheless, previous analyses<sup>16</sup> on a single quantum dot with normal leads based on the finite- $U$  SBFM approach predicted the linear conductance in reasonable agreement with experiments<sup>18</sup> and with numerical renormalization group calculation within the range  $-1.2U \leq \epsilon_d \leq 0.2U$  of the dot level  $\epsilon_d$ , and predicted the magnetic-field-induced peak splitting of nonlinear differential conductance in Kondo regime in qualitatively agreement with experiments<sup>18</sup> and with exact Bethe-ansatz solution<sup>19</sup> in the voltage range up to several multiples of the Kondo temperature  $T_K$ . Even for shot noise the SBFM treatment was shown to yield good result up to the bias voltage  $eV \sim 0.8T_K$ .<sup>20</sup> This indicates that, although the SBFM approach should generally restrict to low temperatures and low voltages ( $eV, T \leq T_K$ ),<sup>20</sup> the finite- $U$  SBFM method can be used to investigate the linear con-

ductance within a relatively wide dot-level range and to study the nonlinear conductance for Kondo systems covering the bias range  $eV$  up to several multiples of  $T_K$ , in which the main magnetic-field and magnetization induced features in Kondo transport appear.

Using the SBMF approach of Kotliar and Ruckenstein<sup>11</sup> we have investigated the linear and nonlinear dc transport in FM/QD/FM systems having finite on-site Coulomb repulsion  $U$ . We find that the Kondo effect shows up as a broad zero-bias resonance in the nonlinear differential conductance versus bias voltage for antiparallel spin alignment in the leads. In parallel configuration, with increasing polarization strength this zero-bias Kondo peak descends and greatly widens by the appearance of shoulders, and finally splits into two peaks on both sides of bias voltage at polarization strength around 0.7 until it disappears at even larger polarization. The linear conductance always drops with enhancing the polarization strength at any spin orientation angle, and exhibits a strong angle variation at large polarization. For a given finite value of polarization, the minimum linear conductance always appears at antiparallel configuration.

## II. FORMULATION

We consider a FM/QD/FM system similar to that discussed by Wang *et al.*<sup>3</sup>: a quantum dot connected to two ferromagnetic leads. When a voltage  $V$  is applied across two leads a current flows through the QD along the  $x$  direction. The magnetic moment of the left lead is pointing to the  $z$  direction,  $\mathbf{M}_L = (0, 0, M)$ , while that of the right lead is at an angle  $\theta$  to the  $z$  axis in the  $y$ - $z$  plane,  $\mathbf{M}_R = (0, M \sin \theta, M \cos \theta)$ . The Hamiltonian of the system can be written as<sup>3</sup>

$$H = H_L + H_R + H_D + H_T. \quad (1)$$

---


$$H_{eff} = \sum_{\sigma} \epsilon_d c_{d\sigma}^{\dagger} c_{d\sigma} + U d^{\dagger} d + \sum_{\alpha=L,R} H_{\alpha} + \lambda^{(1)} \left( \sum_{\sigma} p_{\sigma}^{\dagger} p_{\sigma} + e^{\dagger} e + d^{\dagger} d - 1 \right) + \sum_{\sigma} \lambda_{\sigma}^{(2)} (c_{d\sigma}^{\dagger} c_{d\sigma} - p_{\sigma}^{\dagger} p_{\sigma} - d^{\dagger} d) + \sum_{k,\sigma} [T_{Lk\sigma} C_{Lk\sigma}^{\dagger} c_{d\sigma} z_{\sigma} + T_{Rk\sigma} (\cos \frac{\theta}{2} C_{Rk\sigma}^{\dagger} - \sigma \sin \frac{\theta}{2} C_{Rk\bar{\sigma}}^{\dagger}) c_{d\sigma} z_{\sigma} + h.c.] \quad (5)$$

where three Lagrange multipliers  $\lambda^{(1)}$  and  $\lambda_{\sigma}^{(2)}$  are introduced to take account of the constraints, and in the hopping term the QD fermion operators  $c_{d\sigma}^{\dagger}$  and  $c_{d\sigma}$  are expressed as  $z_{\sigma}^{\dagger} c_{d\sigma}^{\dagger}$  and  $c_{d\sigma} z_{\sigma}$  to recover the many body effect on tunneling.  $z_{\sigma}$  consists of all boson operator sets that are associated with the physical process with which a  $\sigma$ -spin electron is annihilated:

$$z_{\sigma} = (1 - d^{\dagger} d - p_{\sigma}^{\dagger} p_{\sigma})^{-\frac{1}{2}} (e^{\dagger} p_{\sigma} + p_{\bar{\sigma}}^{\dagger} d) (1 - e^{\dagger} e - p_{\bar{\sigma}}^{\dagger} p_{\bar{\sigma}})^{-\frac{1}{2}}. \quad (6)$$

Here

$$H_D = \sum_{\sigma} \epsilon_d c_{d\sigma}^{\dagger} c_{d\sigma} + U c_{d\uparrow}^{\dagger} c_{d\uparrow} c_{d\downarrow}^{\dagger} c_{d\downarrow} \quad (2)$$

describes the QD with a single orbital level  $\epsilon_d$  and a finite on-site Coulomb repulsion  $U$  between electrons;

$$H_{\alpha} = \sum_{k,\sigma} \epsilon_{\alpha k\sigma} C_{\alpha k\sigma}^{\dagger} C_{\alpha k\sigma} \quad (3)$$

stands for the left ( $\alpha = L$ ) or the right ( $\alpha = R$ ) lead with electron energy  $\epsilon_{\alpha k\sigma} = \epsilon_{\alpha k} + \sigma M$ ; and ( $\bar{\sigma} = -\sigma$ )

$$H_T = \sum_{k,\sigma} [T_{Rk\sigma} (\cos \frac{\theta}{2} C_{Rk\sigma}^{\dagger} - \sigma \sin \frac{\theta}{2} C_{Rk\bar{\sigma}}^{\dagger}) c_{d\sigma} + T_{Lk\sigma} C_{Lk\sigma}^{\dagger} c_{d\sigma} + h.c.] \quad (4)$$

describes the tunneling between the QD and the two leads. Note that the small letter symbols  $c_{d\sigma}^{\dagger}$  ( $c_{d\sigma}$ ) and  $c_{\alpha k\sigma}^{\dagger}$  ( $c_{\alpha k\sigma}$ ) are creation (annihilation) operators of electrons in the dot and in the left and right leads with spin up ( $\sigma = 1$  or  $\uparrow$ ) or spin down ( $\sigma = -1$  or  $\downarrow$ ) state in respect to the  $z$ -axis. In the above expressions, the capital letter operator  $C_{Lk\sigma}^{\dagger} = c_{Lk\sigma}^{\dagger}$  for the left lead, while  $C_{Rk\sigma}^{\dagger} = \cos(\theta/2) c_{Rk\sigma}^{\dagger} + \sigma \sin(\theta/2) c_{Rk\bar{\sigma}}^{\dagger}$  for the right lead.

According to the finite- $U$  slave-boson approach,<sup>11</sup> one can use additional four auxiliary boson operators  $e$ ,  $p_{\sigma}$  ( $\sigma = \pm 1$ ) and  $d$ , which are associated respectively with the empty, singly occupied, and doubly occupied electron states of the QD, to describe the above physical problem without interparticle coupling in an enlarged space with constraints: the completeness relation  $\sum_{\sigma} p_{\sigma}^{\dagger} p_{\sigma} + e^{\dagger} e + d^{\dagger} d = 1$  and the particle number conservation condition  $c_{d\sigma}^{\dagger} c_{d\sigma} = p_{\sigma}^{\dagger} p_{\sigma} + d^{\dagger} d$ , ( $\sigma = \pm 1$ ). Within the mean-field scheme we start with the following effective Hamiltonian:

---

From the effective Hamiltonian (5) one can derive four equations of motion of slave-boson operators, which, together with the three constraints, serve as the basic equations. Then we use the mean-field approximation in the statistical expectations of these equations, in which all the boson operators are replaced by their expectation values. In the wide-band limit for the leads the resulting equations are as follows.

$$\sum_{\sigma} \frac{\partial z_{\sigma}}{\partial e} K_{\sigma} + 2\lambda^{(1)} e = 0, \quad (7)$$

$$\sum_{\sigma} \frac{\partial z_{\sigma}}{\partial p_{\sigma'}} K_{\sigma} + 2(\lambda^{(1)} - \lambda_{\sigma'}^{(2)}) p_{\sigma'} = 0, \quad \sigma' = \pm 1, \quad (8)$$

$$\sum_{\sigma} \frac{\partial z_{\sigma}}{\partial d} K_{\sigma} + 2(U + \lambda^{(1)} - \sum_{\sigma} \lambda_{\sigma}^{(2)}) d = 0, \quad (9)$$

$$\sum_{\sigma} |p_{\sigma}|^2 + |e|^2 + |d|^2 = 1, \quad (10)$$

$$\frac{1}{2\pi i} \int d\omega G_{d\sigma\sigma}^{\lessdot}(\omega) = |p_{\sigma}|^2 + |d|^2, \quad \sigma = \pm 1. \quad (11)$$

Here

$$K_{\sigma} \equiv \frac{1}{\pi} \int d\omega \left( z_{\sigma} \text{Re}(G_{d\sigma\sigma}^r) [f_R(\Gamma_{R\sigma} \cos^2 \frac{\theta}{2} + \Gamma_{R\bar{\sigma}} \sin^2 \frac{\theta}{2}) + f_L \Gamma_{L\sigma}] + \sigma z_{\bar{\sigma}} \text{Re}(G_{d\sigma\bar{\sigma}}^r) f_R(\Gamma_{R\sigma} - \Gamma_{R\bar{\sigma}}) \sin \frac{\theta}{2} \cos \frac{\theta}{2} \right), \quad (12)$$

with  $f_{\alpha}(\omega) = 1/(e^{\beta(\omega - \mu_{\alpha})} + 1)$ ,  $\mu_{\alpha}$  the chemical potential of the  $\alpha$ th lead, which is assumed in an equilibrium state at temperature  $1/\beta$ , and  $\Gamma_{\alpha\sigma}(\omega) = 2\pi \sum_{k \in \alpha} |T_{\alpha k \sigma}|^2 \delta(\omega - \epsilon_{\alpha k \sigma})$  the coupling strength function between the QD and the lead  $\alpha$ .  $G_{d\sigma\sigma'}^{r(a)}$  and  $G_{d\sigma\sigma'}^{\lessdot}$  are the elements of the  $2 \times 2$  retarded (advanced) and correlation Green's function matrices  $\mathbf{G}_d^{r(a)}$  and  $\mathbf{G}_d^{\lessdot}$  in the spin space of the QD. The retarded (advanced) Green's function can be written in the form renormalized due to dot-lead couplings,

$$\mathbf{G}_d^{r(a)}(\omega) = \frac{1}{\omega \mathbf{I} - \tilde{\mathbf{H}}_d \pm i\tilde{\mathbf{\Gamma}}} \quad (13)$$

in which  $\mathbf{I}$  is a unit matrix,

$$\tilde{\mathbf{H}}_d = \begin{pmatrix} \tilde{\epsilon}_{d\uparrow} & 0 \\ 0 & \tilde{\epsilon}_{d\downarrow} \end{pmatrix} \quad (14)$$

reflects the dot-level shifting and splitting between spin-up and spin-down electrons,  $\tilde{\epsilon}_{d\sigma} = \epsilon_d + \lambda_{\sigma}^{(2)}$ , and  $\tilde{\mathbf{\Gamma}} = \frac{1}{2}(\tilde{\mathbf{\Gamma}}_L + \tilde{\mathbf{\Gamma}}_R)$  is the effective line width or the renormalized co-tunneling strength, where  $\tilde{\mathbf{\Gamma}}_{\alpha}$  ( $\alpha = L$  or  $R$ ) is a  $2 \times 2$  matrix consisting of elements  $\tilde{\Gamma}_{\alpha}^{11} = |z_{\uparrow}|^2(\Gamma_{\alpha\uparrow} \cos^2 \frac{\theta_{\alpha}}{2} + \Gamma_{\alpha\downarrow} \sin^2 \frac{\theta_{\alpha}}{2})$ ,  $\tilde{\Gamma}_{\alpha}^{22} = |z_{\downarrow}|^2(\Gamma_{\alpha\downarrow} \cos^2 \frac{\theta_{\alpha}}{2} + \Gamma_{\alpha\uparrow} \sin^2 \frac{\theta_{\alpha}}{2})$ , and  $\tilde{\Gamma}_{\alpha}^{12} = \tilde{\Gamma}_{\alpha}^{21} = z_{\uparrow} z_{\downarrow} (\Gamma_{\alpha\uparrow} - \Gamma_{\alpha\downarrow}) \cos \frac{\theta_{\alpha}}{2} \sin \frac{\theta_{\alpha}}{2}$ , where  $\theta_L = 0$  and  $\theta_R = \theta$ . The correlation Green's function  $\mathbf{G}_d^{\lessdot}$  can be obtained with the help of the following relation typical for a noninteracting system:

$$\mathbf{G}_d^{\lessdot} = \mathbf{G}_d^r \mathbf{\Sigma}_d^{\lessdot} \mathbf{G}_d^a, \quad (15)$$

with  $\mathbf{\Sigma}_d^{\lessdot} = i(\tilde{\mathbf{\Gamma}}_L f_L + \tilde{\mathbf{\Gamma}}_R f_R)$ .

The electric current flowing from the left lead into the QD can be obtained from the rate of change of electron number operator of the left lead:<sup>21,22</sup>

$$I_L = \frac{ie}{\hbar} \int \frac{d\omega}{2\pi} \text{Tr} \left\{ \tilde{\mathbf{\Gamma}}_L(\omega) ([\mathbf{G}_d^r(\omega) - \mathbf{G}_d^a(\omega)] f_L(\omega) + \mathbf{G}_d^{\lessdot}(\omega)) \right\}. \quad (16)$$

In the steady transport state, the current flowing from the QD to the right lead must be equal to the current from the left lead to the QD, and the formula (17) can be directly used for calculating the current flowing through the lead-dot-lead system under a bias voltage  $V$  between the two leads:  $I = I_L$ .

### III. NUMERICAL RESULTS AND DISCUSSIONS

We suppose that the left and right leads are made from the identical material and, in the wide band limit, assume constant effective coupling strength  $\Gamma_{L\sigma}(\omega) = \Gamma_{R\sigma}(\omega) = \Gamma_{\sigma}$  respectively for up- and down-spin orientation. The steady state dc current flowing through the system reads

$$I = -\frac{e}{\hbar} \int d\omega \sum_{\sigma} \Gamma_{\sigma} |z_{\sigma}|^2 [2f_L \text{Im}(G_{d\sigma\sigma}^r) + \text{Im}(G_{d\sigma\sigma}^{\lessdot})]. \quad (17)$$

We will take  $\Gamma \equiv (\Gamma_{\uparrow} + \Gamma_{\downarrow})/2$  as the energy units in the following and define the spin polarization as  $P \equiv$

$(\Gamma_{\uparrow} - \Gamma_{\downarrow})/(2\Gamma)$ . The Kondo temperature in the case of  $P = 0$ , given by  $T_K^0 = U\sqrt{\beta} \exp(-\pi/\beta)/2\pi$  with  $\beta = -2U\Gamma/\epsilon_d(U + \epsilon_d)$ , will be used as the dynamical energy scale in presenting the nonlinear conductance.

In the following we will deal with FM/QD/FM systems having a fixed finite Coulomb repulsion  $U = 6$  and consider effects of changing bare dot level  $\epsilon_d$ , polarization strength  $P$  and relative spin orientation  $\theta$ .

In calculating the dc current from Eq.(17) under a finite bias voltage  $V$  between the two leads, we choose the energy zero such that the chemical potential  $\mu_L = -\mu_R = eV/2$  for the left and right leads for convenience.

Linear conductance  $G = (dI/dV)_{V=0}$  is related to the slave-boson parameters  $e^2, p_{\sigma}^2, d^2, \lambda^{(1)}, \lambda_{\sigma}^{(2)}$  and  $|z_{\sigma}|^2$  at zero bias. In antiparallel configuration ( $\theta = \pi$ ), all the slave-boson parameters are identical for up and down spin indices and independent of  $P$ . In the parallel configuration ( $\theta = 0$ ),  $p_{\sigma}^2, \lambda_{\sigma}^{(2)}$  and  $|z_{\sigma}|^2$  split for up and down spins and all the parameters exhibit strong  $P$ -dependence. As an example we plot in Fig.1 the zero-bias parameters  $e^2, p_{\sigma}^2, d^2, \lambda^{(1)}, \lambda_{\sigma}^{(2)}$  and the average electron

number in the dot  $n = p_{\uparrow}^2 + p_{\downarrow}^2 + 2d^2$  in the parallel configuration at zero temperature for the case of  $\epsilon_d = -1$  and  $U = 6$ .

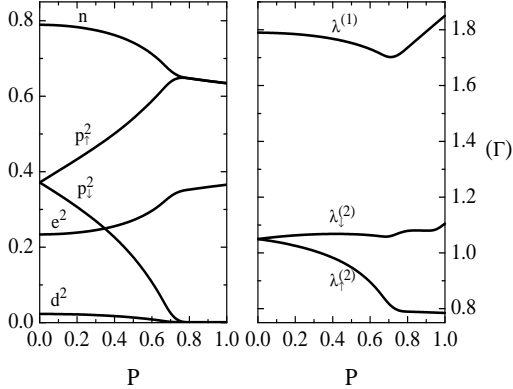


FIG. 1. The expectation values of slave-boson operators  $e^2, d^2, p_{\uparrow}^2, p_{\downarrow}^2$ , the corrections of the renormalized dot level  $\lambda_{\uparrow}^{(1)}, \lambda_{\downarrow}^{(1)}, \lambda_{\uparrow}^{(2)}, \lambda_{\downarrow}^{(2)}$ , and the electron number dwelling in the dot  $n = p_{\uparrow}^2 + p_{\downarrow}^2 + 2d^2$ , are shown as functions of polarization  $P$  at zero temperature and zero bias voltage  $V = 0$ . The quantum-dot in the FM/QD/FM system has a single bare energy level  $\epsilon_d = -1$  and a finite on-site Coulomb repulsion  $U = 6$ .

Figs. 2 and 3 show the zero-temperature linear conductance  $G$  as a function of the bare energy level  $\epsilon_d$  of the quantum-dot having a fixed on-site Coulomb repulsion  $U = 6$  at different polarizations  $P = 0, 0.3, 0.5, 0.7$  and  $0.9$  on two leads in parallel ( $\theta = 0$ ) and in antiparallel ( $\theta = \pi$ ) configurations. Each curve covers three regimes, containing the resonance peak due to the dot level around  $\epsilon_d = 0$ , the charging peak around  $\epsilon_d = -U$ , and the Kondo peak centered at  $\epsilon_d = -U/2$ . In the case of zero polarization  $P = 0$  and in the antiparallel configuration of arbitrary polarization, all the slave-boson parameters are identical for up and down spin indices, and electrons with up-spin and down-spin are equally available in the whole lead-dot-lead system, favoring the formation of the Kondo-correlated state within a relatively wide dot level range centered at  $\epsilon_d = -3$ . At the same time, since there is no splitting of the renormalized dot levels  $\tilde{\epsilon}_{d\sigma}$  for up and down spins, the resonance and charging peaks are relatively narrow. The  $G$ -vs- $\epsilon_d$  curves appear to be smooth hump-type structures. On the other hand, since there is no spin-flip mechanism in the tunneling coupling and in the antiparallel configuration the available minority-spin (e.g. up-spin) states in the right lead decrease with increasing polarization strength, the transfer of the majority-spin (up-spin) electrons from the left lead to the right lead is suppressed by the finite  $P$ , such that the conductance of the system goes down with increasing  $P$  and vanishes at  $P = 1$ . In the parallel configuration, finite polarization  $P > 0$  splits the dot level for up and down spins and thus broadens the resonance peaks around  $\epsilon_d = 0$  and  $\epsilon_d = -U$ . At the same time the central Kondo peaks is progressively narrowed with in-

creasing  $P$  due to the decrease of the available minority-spin electrons in the two leads. This two factors lead to the appearance of kinks or splitting peaks in the  $G$ -vs- $\epsilon_d$  curves for  $P = 0.3, 0.5, 0.7$  and  $0.9$  in the parallel configuration. Nevertheless, the unitary limit  $G = 2e^2/h$  can still be reached as long as  $P < 1$ . In the case of  $P = 1$ , since there is no minority-spin electron in the leads, the formation of the Kondo-correlated state is impossible and the double occupancy probability of the dot level vanishes,  $d^2 = 0$ . In this case the Kondo peak disappears, together with the charging peak. There remains only a tunneling peak centered around  $\epsilon_d = 0$  in the  $G$ -vs- $\epsilon_d$  curve, which stems from the up-spin electrons.

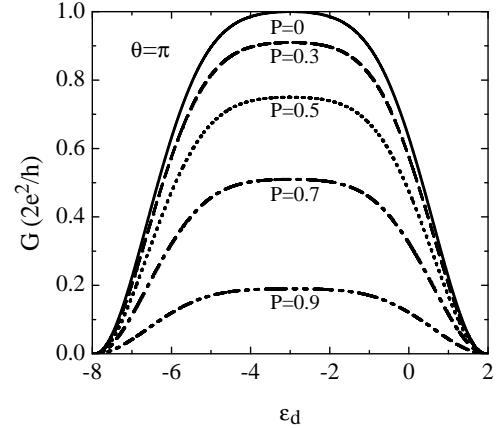


FIG. 2. The linear conductance  $G$  of FM/QD/FM systems is shown as a function of the bare dot level  $\epsilon_d$  for different spin polarization  $P$  of the leads in the antiparallel configuration ( $\theta = \pi$ ). The dot has a finite on-site Coulomb repulsion  $U = 6$ .

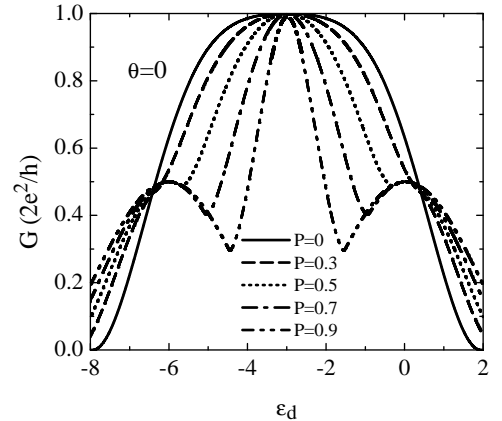


FIG. 3. The linear conductance  $G$  of FM/QD/FM systems is shown as a function of the bare dot level  $\epsilon_d$  for different spin polarization  $P$  of the leads in the parallel configuration ( $\theta = 0$ ). The dot has a finite on-site Coulomb repulsion  $U = 6$ .

Fig. 4 shows the calculated zero-temperature linear

conductance  $G$  for a FM/QD/FM system having  $\epsilon_d = -2$  and  $U = 6$  as a function of polarization  $P$  at several different spin orientations  $\theta = 0, \pi/4, \pi/2, 3\pi/4$ , and  $\pi$ . For each fixed orientation the linear conductance decreases with increasing  $P$  straightforwardly from the maximum value  $G = 1.97e^2/h$  at  $P = 0$  down to its minimum. The conductance descends generally faster at larger  $\theta$  except for the case of  $\theta = \pi/4$  and  $P > 0.75$ , where  $G$  goes down slower than that of  $\theta = 0$ . This can be understood as due to the rapid decrease of the conductance (or the swift narrowing of the Kondo peak) with  $P$  increasing in the parallel configuration, as seen in Fig. 3. For a given large  $P$  when rotating an angle  $\pi/4$  from parallel configuration, the conductance increase due to the reduction of the equivalent parallel polarization from  $P$  to  $P \cos(\pi/4)$  overcompensates the conductance decrease induced by applying an equivalent polarization  $P \sin(\pi/4)$  along  $\theta = \pi/2$ . In Fig. 5 we plot the linear conductance  $G$  versus the angle  $\theta$  of the relative spin orientation at various polarization strengths  $P = 0, 0.3, 0.5, 0.7$  and  $0.9$  for the same system as described in Fig. 4. We see a clear angle variation of the linear conductance at a finite spin polarization, with the minimum always at  $\theta = \pi$ . At small  $P$  the conductance  $G$  reaches its maximum at  $\theta = 0$ , but at large polarization the maximum appears near  $\theta = \pi/4$ .

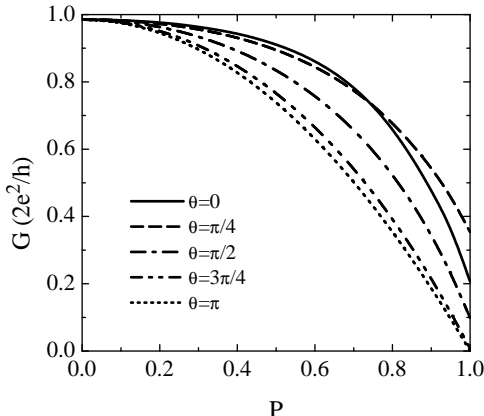


FIG. 4. The linear conductance  $G$  is shown as a function of polarization  $P$  for different spin orientation  $\theta$  at zero temperature. The system has a single bare dot level  $\epsilon_d = -2$  and a finite on-site Coulomb repulsion  $U = 6$ .

Fig. 6 shows the calculated differential conductance  $dI/dV$  versus the bias voltage under antiparallel configuration ( $\theta = \pi$ ) at various polarizations  $P = 0, 0.3, 0.5, 0.7$  and  $0.9$  for a FM/QD/FM system having a single dot level  $\epsilon_d = -1$  and a finite on-site Coulomb repulsion  $U = 6$  ( $T_K^0 = 0.4$ ). All the curves exhibit a single zero-bias peak having essentially the same width but with peak height going straight down with growing  $P$  from the highest value  $1.79e^2/h$  at  $P = 0$ . As pointed above, in antiparallel configuration electrons with up-spin and down-spin are equally available in the lead-dot-lead sys-

tem, in favor of the formation of the Kondo-correlated state for all values of  $P$ . However, since the up-spin states are almost unavailable in the right lead in the case of large polarization  $P$ , the transfer of electrons (almost up-spins) from the left lead to the right lead is largely suppressed. The conductance of the system goes down to zero with increasing  $P$  to 1.

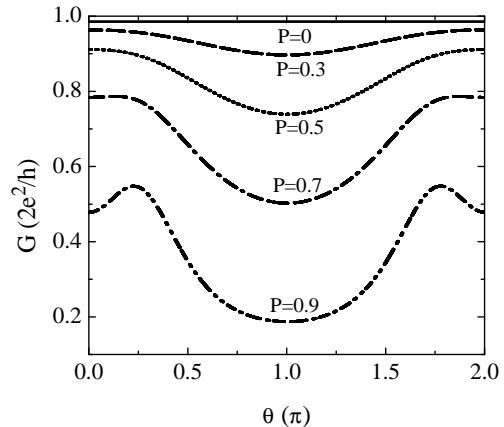


FIG. 5. The linear conductance  $G$  versus the relative spin polarization angle  $\theta$  at different polarization strength  $P$  for the same system as described in Fig. 4.

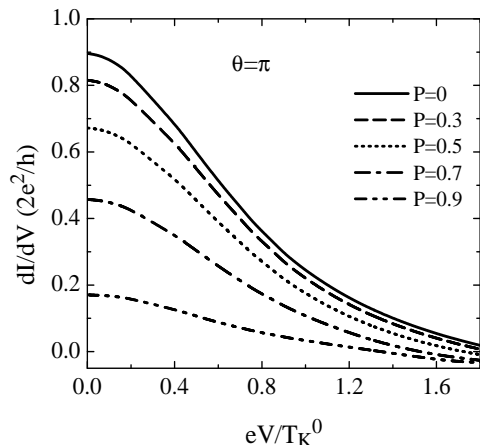


FIG. 6. Zero-temperature differential conductance  $dI/dV$  versus the bias voltage  $eV$  at different polarization  $P$  in the antiparallel spin configuration ( $\theta = \pi$ ). The quantum-dot in the FM/QD/FM system has a single bare energy level  $\epsilon_d = -1$  and a finite on-site Coulomb repulsion  $U = 6$ .

The situation becomes different in the case of parallel configuration, where the available down-spin electrons are less than the up-spin ones in the leads when  $P > 0$ . Although the former can still provide screening for dot electrons to form Kondo correlation to certain degree at small values of  $P$ , the effect gradually weakens with growing  $P$  for this  $\epsilon_d = -1$  system (somewhat away from the unitary limit), leading to the decrease in

linear conductance from the peak value at  $P = 0$ . In the case of large polarization, the number of minority-spin electrons is too small to form the Kondo-correlation state and Kondo-induced conductance enhancement disappears rapidly with  $P$  increasing. On the other hand, even when there is no down-spin states ( $P = 1$ ), the up-spin states are always available in both left and right leads, allowing the up-spin electrons to carry a current through tunneling. Fig.7 illustrates the calculated differential conductance  $dI/dV$  for  $\theta = 0$  at various polarizations  $P = 0, 0.3, 0.5, 0.7$  and  $0.9$ . We can see that the zero-bias Kondo peak in the  $dI/dV$ -vs- $eV$  curve of  $P = 0$ , descends and widens by the appearance of shoulders on both sides of bias voltage at  $P = 0.3$  and  $P = 0.5$ . This is apparently due to the weakening of the Kondo correlation and the splitting of the renormalized dot level  $\tilde{\epsilon}_d$  (see Fig.1). At  $P = 0.7$ , the level splitting is large enough and there are still sufficient down-spin electrons for the formation of Kondo state, we see the splitting of the zero-bias anomaly into two peaks on both sides of the applied voltage at a distance around twice the renormalized level splitting ( $\lambda_{\downarrow}^{(2)} - \lambda_{\uparrow}^{(2)} \approx 0.27$ ) (see Fig.1). At  $P = 0.8$ , almost no down-spin electron exists in the dot and no Kondo-related  $dI/dV$  behavior shows up for this  $\epsilon_d = -1$  system.

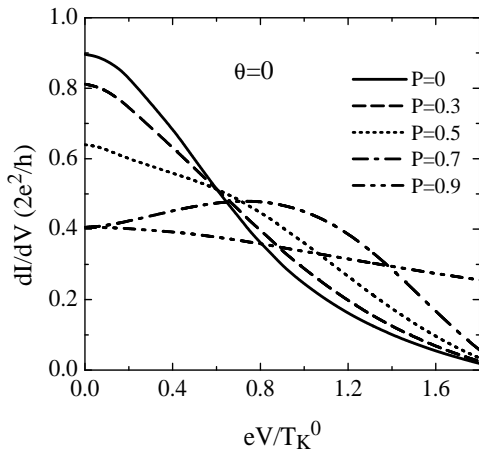


FIG. 7. Zero-temperature differential conductance  $dI/dV$  versus the bias voltage  $eV$  at different polarization  $P$  in the parallel spin configuration ( $\theta = 0$ ). The quantum-dot in the FM/QD/FM system has a single bare energy level  $\epsilon_d = -1$  and a finite on-site Coulomb repulsion  $U = 6$ .

Similar trend can also be seen in Fig. 8, where we plot the differential conductance  $dI/dV$  versus the bias voltage  $eV$  in the case of  $P = 0.8$  at various relative spin orientations  $\theta = 0, \pi/4, \pi/2, 3\pi/4$  and  $\pi$ . At this strength of polarization, there is no Kondo-correlated state to appear for the  $\epsilon_d = -1$  system in the parallel configuration ( $\theta = 0$ ). In the case of  $\theta = \pi/4$ , however, the dot level splitting is large enough and there are sufficient down-spin electrons to survive the reduced effective parallel polarization  $P \cos(\pi/4)$  for the formation of the Kondo

correlation. A clear appearance of nonzero-bias maximum in the voltage-dependent conductance can be seen.

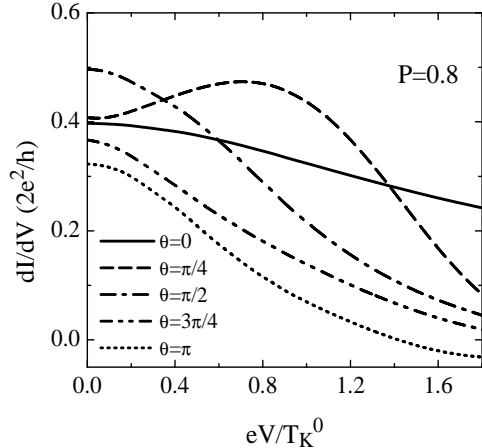


FIG. 8. Zero-temperature differential conductance  $dI/dV$  versus the bias voltage  $eV$  at different spin orientation  $\theta$  for polarization strength  $P = 0.8$ . The quantum-dot in the FM/QD/FM system has a single bare energy level  $\epsilon_d = -1$  and a finite on-site Coulomb repulsion  $U = 6$ .

In spite of dealing with the same system ( $U = 6$  and  $\epsilon = -1$ ), the behavior of the linear and nonlinear conductance obtained here is quite different from that reported in Ref. 7. In parallel configuration, our predicted linear conductance  $G$  goes down with increasing  $P$  at least up to  $P = 0.7$  (see Fig.7) in contrast to their  $G$  which increases with rising  $P$  (Fig.5a in Ref. 7). In the bias-dependent differential conductance our results show the clear trend of the zero-bias peak broadening with increasing  $P$  and finally splitting at large  $P$  under parallel and nearly parallel spin alignments due to the splitting of the renormalized dot level, while Ref. 7 predicts a single zero-bias peak narrowing with growing  $P$ . In antiparallel configurations we obtain a much wider zero-bias peak in nonlinear differential conductance than theirs. Our predicted splitting of the zero-bias anomaly in nonlinear differential conductance under parallel and nearly parallel spin alignments for large  $P$ , is in general agreement with Refs. 9, 10 in the large  $U$  limit. However, in both parallel and antiparallel configurations, the zero-bias peaks and the split peaks seen in the voltage-dependent differential conductance in the present investigation are broader than those reported in Refs. 9, 10. It should be noted that the present analysis yields a smaller dot-level splitting than theirs. For instance, for systems with  $U = \infty$ ,  $\epsilon_d = -2$ , Ref. 9 reported a distance  $e\Delta V$  around 0.5 between the split peaks in the voltage-dependent differential conductance in the parallel configuration at a polarization strength of  $P = 0.2$ , that is about the same split-peak distance obtained at  $P = 0.6$  in this paper for the system of  $U = 6$  and  $\epsilon_d = -1$ .

#### IV. SUMMARY

We have theoretically investigated the linear and non-linear electron transport of a spin-valve system consisting of a quantum dot connected to two ferromagnetic leads in Kondo regime but somewhat apart from the unitary limit. Based on the finite- $U$  slave-boson mean field approach we find markedly different transport behavior when changing the relative spin orientation. In the antiparallel configuration where electrons with up-spin and down-spin are equally available in the system, a single zero-bias Kondo peak always appears in the voltage-dependent differential conductance through the whole range of polarization  $0 \leq P < 1$ , but the peak height drops down with increasing  $P$  and vanishes at  $P = 1$ . In the parallel configuration, with increasing the spin polarization from zero, Kondo peak descends and greatly widens by the appearance of shoulders and finally splits into two peaks on both sides of bias voltage at polarization around  $P \sim 0.7 - 0.8$ , until disappears at even larger  $P$ . At any spin alignment angle, the linear conductance generally drops with increasing spin polarization. It is shown that a Kondo-dominant FM/QD/FM system may exhibit strong angle variation in linear conductance at large polarization, forming an effective spin valve.

We would like to thank Dr. S.Y. Liu and Dr. W.S. Liu for helpful discussions. This work was supported by the National Science Foundation of China, the Special Funds for Major State Basic Research Project, and the Shanghai Municipal Commission of Science and Technology.

- <sup>1</sup> M.N. Baibich, J.M. Broto, A. Fert, F. Nguyen Van Dau, F. Pteroff, P. Etienne, G. Creuzet, A. Friederich, and J. Chazelas, *Phys. Rev. Lett.* **61**, 2472 (1988).
- <sup>2</sup> M. Julliere, *Phys. Lett.* **54 A**, 225 (1975).
- <sup>3</sup> Baigeng Wang, Jian Wang, and Hong Guo, *J. Phys. Soc. Jpn* **70**, 2645 (2001).
- <sup>4</sup> K. Tsukagoshi, B.W. Alphenaar, and H. Ago, *Nature* **401**, 573 (1999).
- <sup>5</sup> L. Sheng, Y. Cheng, H.Y. Teng, and C.S. Ting, *Phys. Rev. B* **59**, 480 (1999).
- <sup>6</sup> G.A. Prinz, *Science* **282**, 1660 (1998).
- <sup>7</sup> N. Sergueev, Qing-feng Sun, Hong Guo, B.G.Wang and Jian Wang, *Phys. Rev. B* **65**, 165303 (2002).
- <sup>8</sup> T.K. Ng, *Phys. Rev. Lett.* **70**, 3635 (1993).
- <sup>9</sup> J. Martinek, Y. Utsumi, H. Imamura, J. Barnaś, S. Maekawa, J. König, and G. Schön, cond-mat/0210006.
- <sup>10</sup> Rong Lü and Zhi-Rong Liu, cond-mat/0210350.
- <sup>11</sup> G. Kotliar and A.E. Ruckenstein, *Phys. Rev. Lett.* **57**, 1362 (1986).
- <sup>12</sup> P. Coleman, *Phys. Rev. B* **29**, 3035 (1984).
- <sup>13</sup> T. Aono et al. *J. Phys. Soc. Jpn.* **67**, 1860 (1998).
- <sup>14</sup> Georges and Y. Meir, *Phys. Rev. Lett.* **82**, 3508 (1999).
- <sup>15</sup> R. Aguado and D.C. Langreth, *Phys. Rev. Lett.* **85**, 1946 (2000).
- <sup>16</sup> Bing Dong and X.L. Lei, *J. Phys: Condens. Matter* **13**, 9245 (2001); *Phys. Rev. B* **63**, 235306 (2001).
- <sup>17</sup> Bing Dong and X.L. Lei, *Phys. Rev. B* **65**, 241304 (2002).
- <sup>18</sup> D. Goldhaber-Gordon, H. Shtrikman, D. Mahalu, D. Abusch-Magder, U. Meirav, and M.A. Kastner, *Nature (London)* **391**, 156 (1998).
- <sup>19</sup> J.E. Moore and X.G. Wen, *Phys. Rev. Lett.* **85**, 1722 (2000).
- <sup>20</sup> Y. Meir and A. Golub, *Phys. Rev. Lett.* **88**, 116802 (2002).
- <sup>21</sup> Y. Meir and N.S. Wingreen, *Phys. Rev. Lett.* **68**, 2512 (1992).
- <sup>22</sup> A.P. Jauho, N.S. Wingreen, and Y. Meir, *Phys. Rev. B* **50**, 5528 (1994)